Evolution of fission properties in Fermium region

T. M. Shneidman
A. Rahmatinejad, A.V. Andreev, A. V. Isaev, R. S. Mukhin

May, 2026

Bogoliubov Laboratory of Theoretical Physics,
Joint Institute for Nuclear Research

Separator for Heavy Element Spectroscopy – SHELS

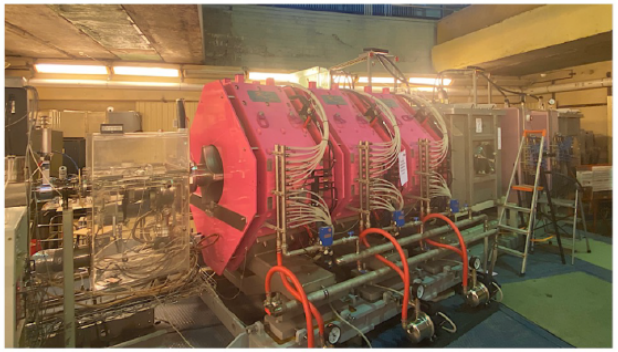

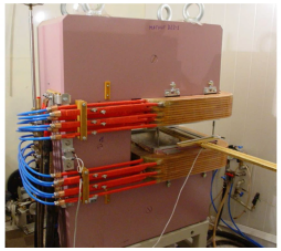

Popeko A. G. et al.
Separator for Heavy ELement Spectroscopy – velocity filter SHELS
NIM B 376 (2016) 140–143

Principal components of SHELS.

Quadrupole lenses	
Maximum field gradient	13 T/m
Effective length	38 cm
Aperture radius	10 cm
Electrostatic deflectors	
Maximum field gradient	40 kV/cm
Effective length	65.7 cm
Distance between plates	10–20 cm
Nominal deflection angle	8°
Magnetic dipoles D22-1,2	
Maximum field strength	0.8 T
Effective length	59.7 cm
Gap height	13.5 cm
Nominal deflection angle	22°
Magnetic dipole D8	
Maximum field strength	0.2 T
Effective length	58.8 cm
Gap height	14 cm
Nominal deflection angle	8°

SFiNx – Spontaneous Fission, Neutrons and x-rays

$\varepsilon_n = 55\pm1\%$

Isaev A. V. et al.
The SFiNx detector system
PEPAN Letters 19 (2022)
P. 37–45

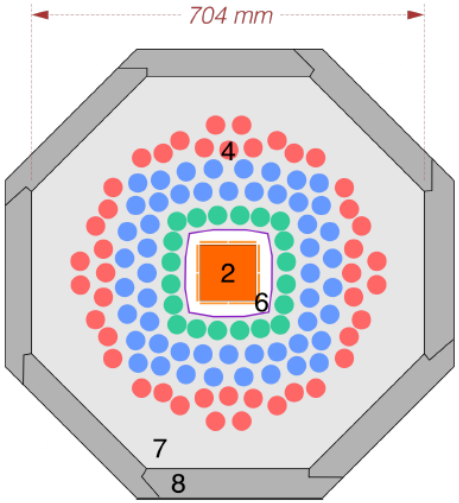

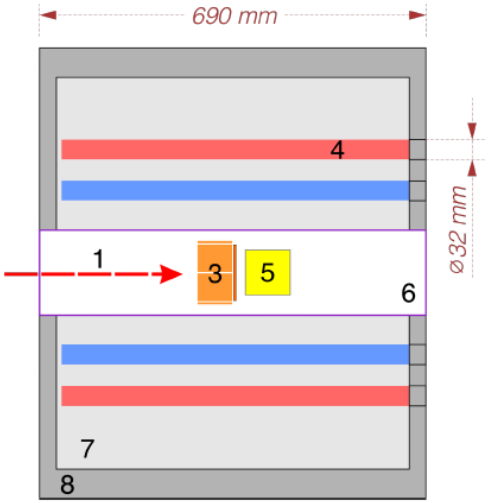

The legend:

1 – evaporation residues
2 – focal-plane Si-detector
3 – side Si-detectors
4 – ^{3}He-counters
5 – scintillator
6 – vacuum chamber
7 – moderator
8 – shield

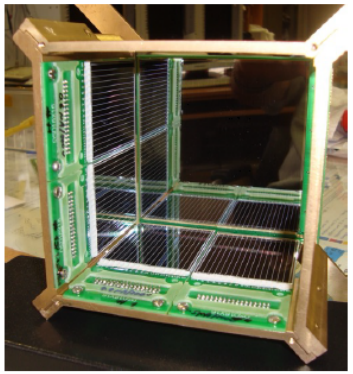

DSSD 100×100 mm
128×128-strips

Measured and restored spectra

The true form of the neutron multiplicity distribution can be restored using Tikhonov's method of statistical regularization of inverse ill-posed problems.

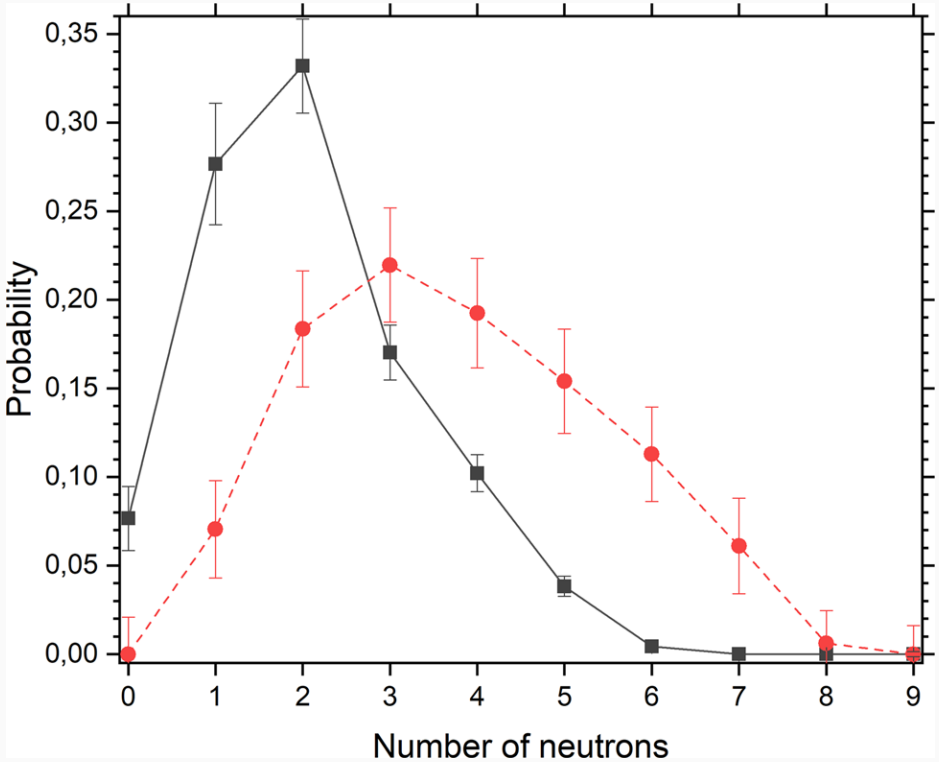

R.S. Mukhin et al., Phys. Part. Nucl. Lett. 18(4), 439–444 (2021).
V. F. Turchin, V. P. Kozlov, and M. S. Malkevich, Sov. Phys. Usp. 13, 681 (1970).

Systematics of neutron multiplicities

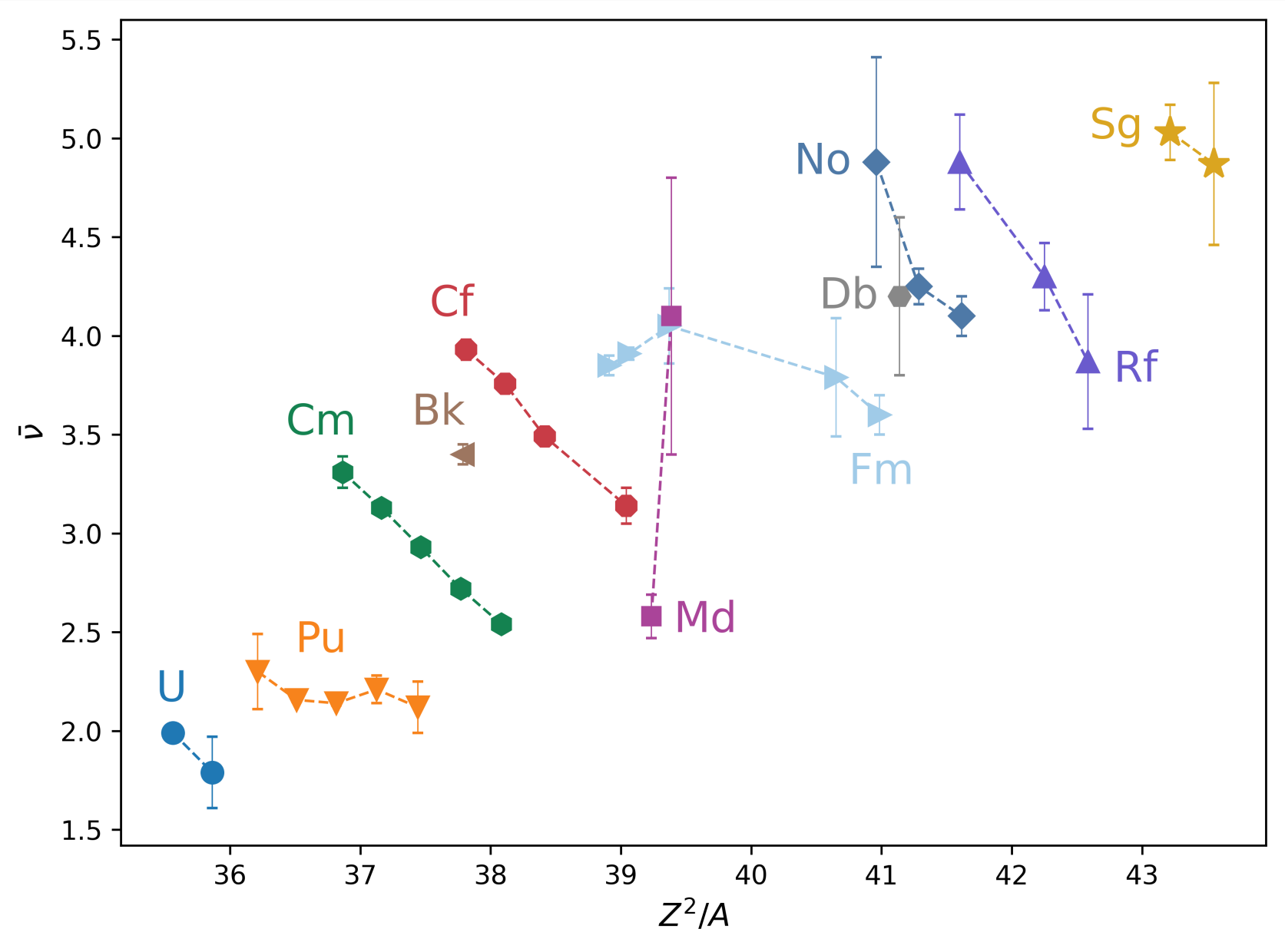

Shapes of the Prompt Neutron Multiplicity Distributions

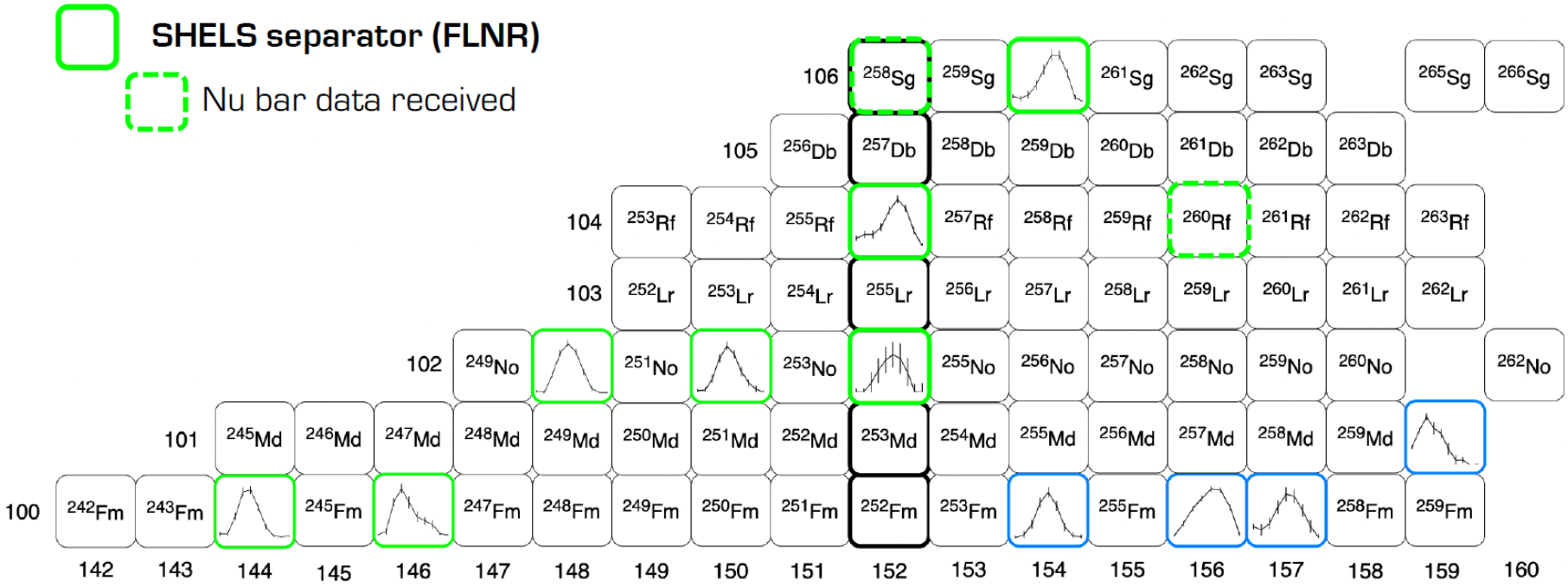

A.V. Isaev, et al., submitted to PRC. (JINR preprint E7-2026-3)
https://www1.jinr.ru/Preprints/2026/03(E7-2026-3).pdf
R.S. Mukhin et al., Eur. Phys. J. A **60**, 223 (2024).
R.S. Mukhin et al., CPC **48**, 064002 (2024).
A.V. Isaev, et al., PLB **843**, 138008 (2023).
A. V. Isaev, EPJA, **58** 108 (2022).

DNS approach for description of spontaneous fission

- After crossing the fission barrier, the fissioning nucleus is treated as a superposition of various dinuclear systems.
- DNS is a system of two fragments in touching configuration characterized by their charges, masses, and deformations.
- The potential energy of DNS as a function of relative distance coordinate *R* has a pocket in the vicinity of touching configuration.
- The decay of DNS competes with an evolution in mass/charge asymmetry coordinates and in deformation of the fragments.

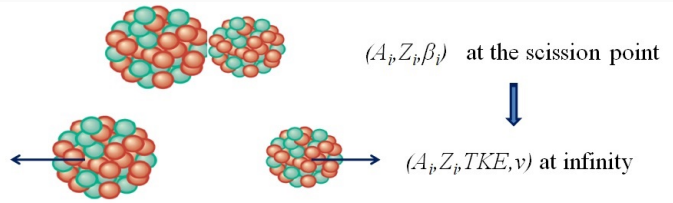

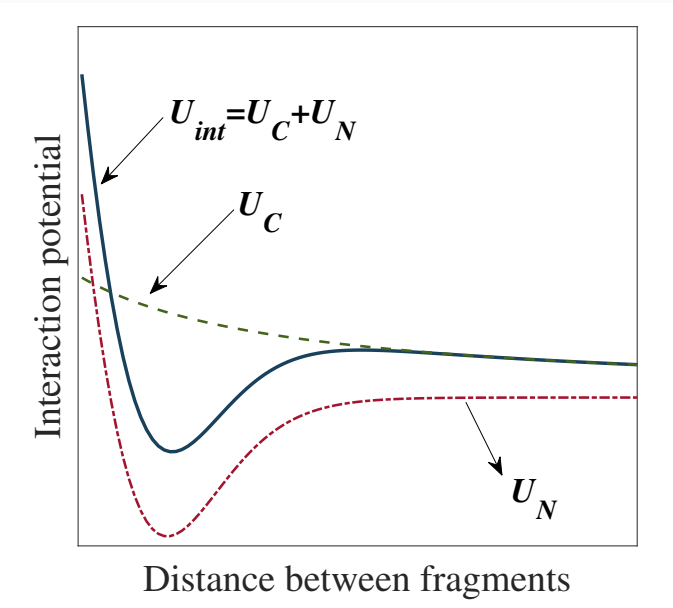

Density of dinuclear system: $^{232}\mathrm{Th} \longrightarrow {}^{132}\mathrm{Sn}(0.0) + {}^{100}\mathrm{Zr}(0.3)$

DNS density at the distance R between the fragments:

$$\rho(\mathbf{r}) = \rho_1(\mathbf{r}) + \rho_2(\mathbf{r} - \mathbf{R})$$

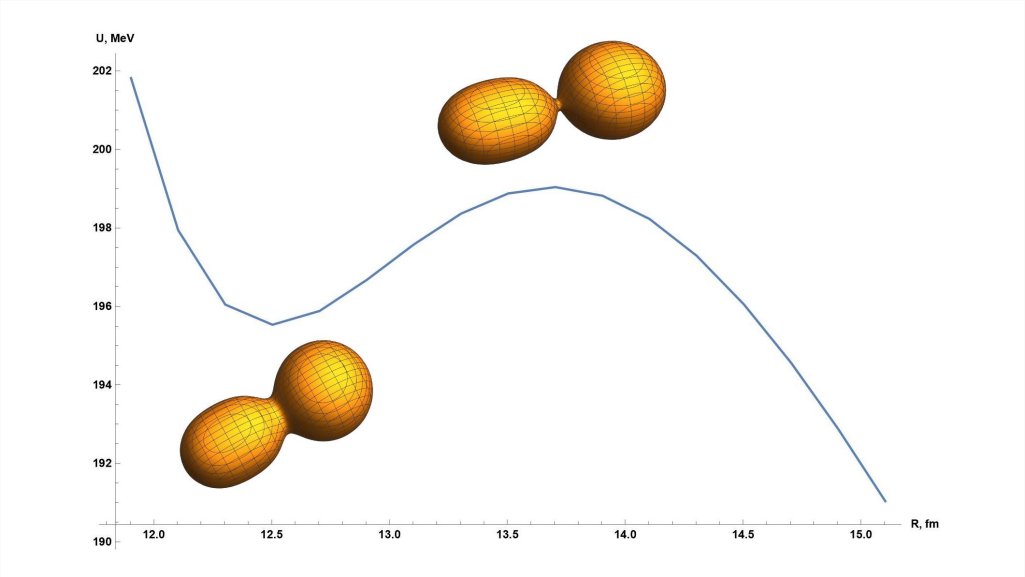

- The necked-in configuration of the fissioning nucleus can be viewed as a dinuclear system in a touching configuration.
- Near the top of the fission barrier, where the neck practically disappears, the nuclear interaction becomes weak $\longrightarrow$ the system accelerates rapidly toward scission.
- The fission observables are determined mainly by the DNS configuration in the pocket of the nucleus–nucleus potential (at touching).

Evolution of fissioning nucleus after crossing the fission barrier

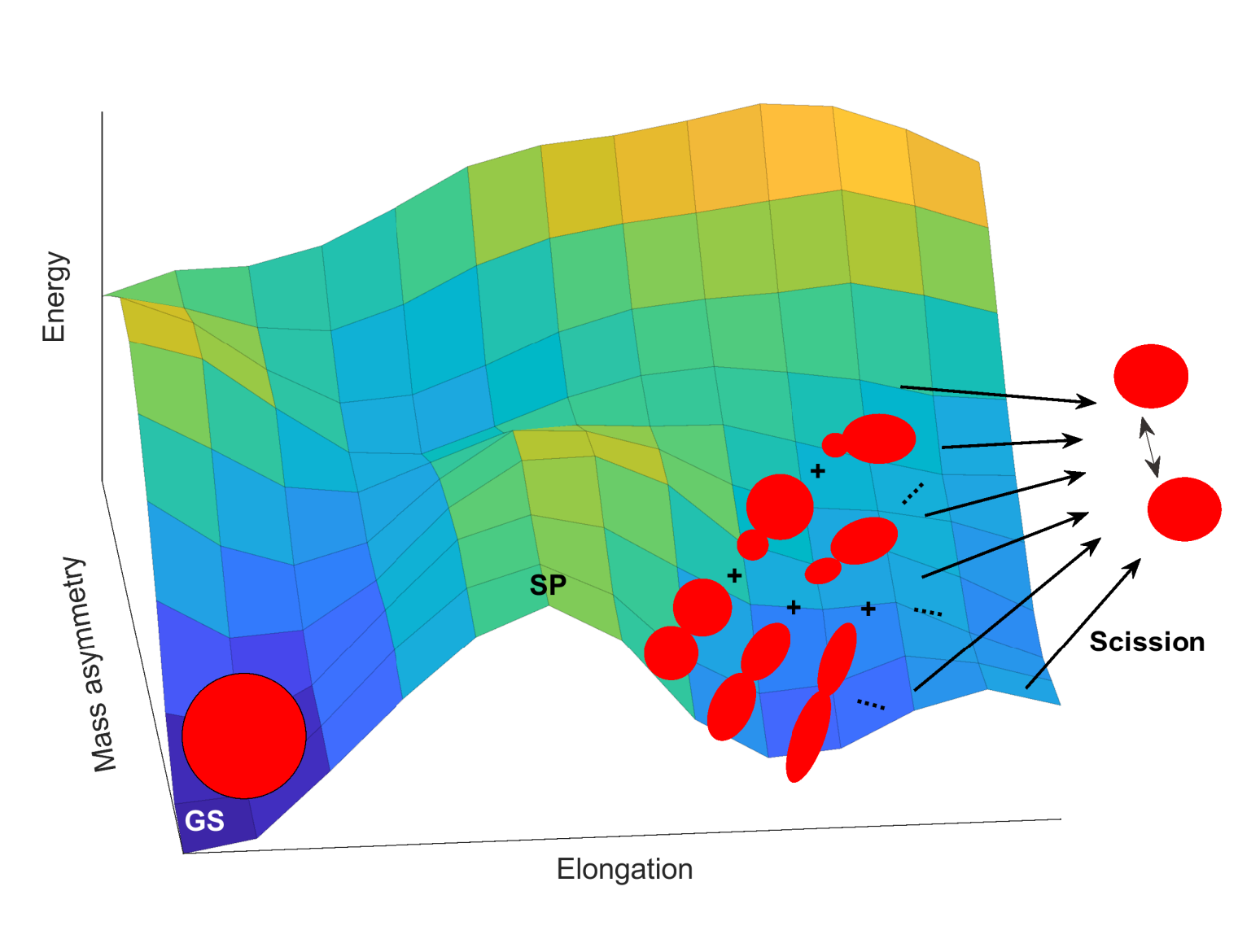

Evolution of fissioning nucleus after crossing the fission barrier

The evolution of DNS distribution in time is described using the master equation:

$$n = (Z_1, A_1, \beta_1, Z_2, A_2, \beta_2).$$

$$\frac{dP(n)}{dt} = \sum_{n' \neq n} \Lambda(n'|n)P(n') - \sum_{n' \neq n} \Lambda(n|n')P(n) - \Lambda_d(n)P(n)$$

$P(n)$ – Probability that the system is in the state n.
$P_0(n) = P(n, t = 0)$ – Probabilities of initially-formed DNS.
$\Lambda(n|n')$ – Transition rates for switching from n to n'.
$\Lambda_d(n)$ – Decay rates.

The distribution of primary fission fragments

$$P_f(n[Z_1, A_1, \beta_1, Z_2, A_2, \beta_2])$$

is obtained with Monte-Carlo technique.

Potential energy of the DNS

The contribution of different DNS is determined by its potential energy: larger potential energy $\longrightarrow$ smaller excitation energy $\longrightarrow$ smaller probability

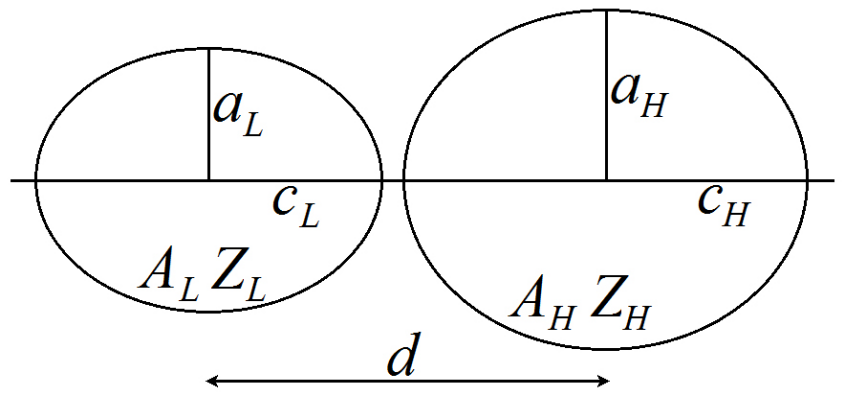

$$U_{sc}(\beta_L, \beta_H, d) = U_{LD}(\beta_{L,H}) + \delta U_{sh}(\beta_{L,H}) + V^C(\beta_{L,H}, d) + V^N(\beta_{L,H}, d)$$

- U_{LD}: Liquid-drop energy
- δU_{sh}: Shell correction
- V^C: Coulomb interaction
- V^N: Nuclear interaction

A.V. Andreev et al., EPJ A **30**, 579 (2006).

Nuclear interaction energy

Double folding potential: (G. G. Adamian *et al.*, IJMPE **5**, 191 (1996).)

$$V^N(d) = \int \rho_1(\mathbf{r}_1)\rho_2(\mathbf{d}-\mathbf{r}_2)F(\mathbf{r}_1-\mathbf{r}_2)\mathrm{d}\mathbf{r}_1\mathrm{d}\mathbf{r}_2,$$

with the density-dependent forces (Migdal forces):
A. B. Migdal, *Theory of finite Fermi Systems...* (Nauka, Moscow, 1982).

$$F(\mathbf{r}_1-\mathbf{r}_2) = C_0\left(F_{in}\frac{\rho_0(\mathbf{r}_1)}{\rho_{00}} + F_{ex}\left(1-\frac{\rho_0(\mathbf{r}_1)}{\rho_{00}}\right)\right)\delta(\mathbf{r}_1-\mathbf{r}_2),$$

$F_{in,ex} = (f_{in,ex} + f'_{in,ex}\tau_1\cdot\tau_2) + (g_{in,ex} + g'_{in,ex}\tau_1\cdot\tau_2)\sigma_1\cdot\sigma_2$
$C_0 = 300\ \mathrm{MeV\ fm}^3$, $f_{in,ex} = 0.09(-2.59)$, $f'_{in,ex} = 0.42(0.54)$

$$\rho_0(\mathbf{r}) = \rho_1(\mathbf{r}) + \rho_2(\mathbf{r}).$$

Densities are in the form of Fermi distribution.

Potential energy of DNS as a function of the fragment deformations.

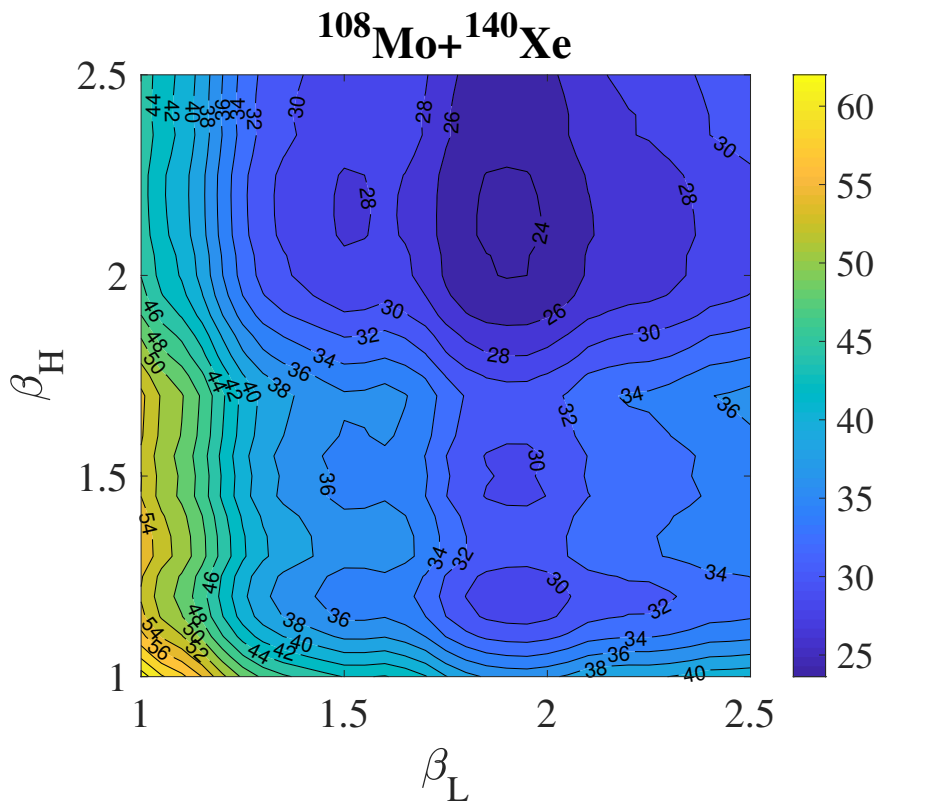

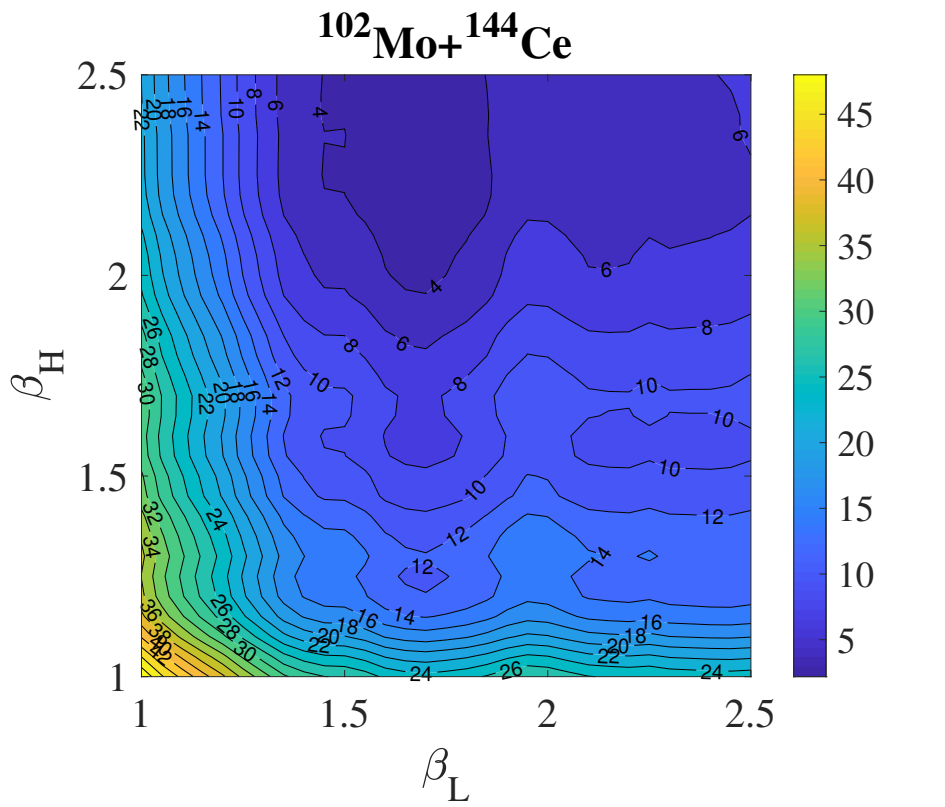

Complex structure of the PES (one or several local minima) is due to the shell correction of fragments.

Transition rates

The transition rates are expressed in terms of the microscopic transition probabilities and of the level densities of the final state.

$$\Lambda(n|n') = \lambda_{nn'}\rho(E^*_{n'}, n'), \quad \Lambda(n'|n) = \lambda_{n'n}\rho(E^*_n, n)$$

$$\lambda_{n'n} = \lambda_{nn'} = \lambda^{(i)}/\sqrt{\rho(n')\rho(n)}; \quad i = (m.a., \beta)$$

$$\Lambda_d(n) = \lambda_d\rho_{s.p.}(E^* - V_B, n)$$

$$\lambda_d = \begin{cases} 1/\sqrt{\rho_{s.p.}(n)\rho(n)}, & \text{if } (E^* > V_B) \\ 0, & \text{if } (E^* < V_B) \end{cases}$$

L.G. Moretto and J.S. Sventek, Phys. Lett. B **58**, 26 (1975).
G.G. Adamyan, A.K. Nasirov, N.V. Antonenko, R.V. Jolos , Fiz. Elem. Chastits At.Yadra **25**, 1379 (1994).

Level densities of DNS

The intrinsic level density (LD) of DNS:

$$\rho_{int}(E^*, n) = \int \rho_1(A_1, Z_1, \beta_1, \varepsilon)\rho_2(A_2, Z_2, \beta_2, E^* - \varepsilon)\mathrm{d}\varepsilon.$$

The LD of DNS fragments is calculated in superfluid formalism.

The DNS level density is obtained as a folding of intrinsic LD and the density of collective states:

$$\rho(E^*, n) = \sum_x \rho_{int}(E^* - E_x^n, n).$$

P. Decowski, et al., Nucl. Phys. A **110**, 129 (1968).
A. Bezbakh, et al., EPJA **52**, 353 (2015).
A. Rahmatinejad, et al., PRC **101**, 054315 (2020)/ **103**, 034309 (2021)/ **105**, 044328 (2022).

Choice of distribution of initial states

We choose the systems whose mass quadrupole moment lies in the interval of 10% around the value of quadrupole moment of ellipsoid with axis ratio $a : b$.

$Q_2^{ellips} \sim a : b$

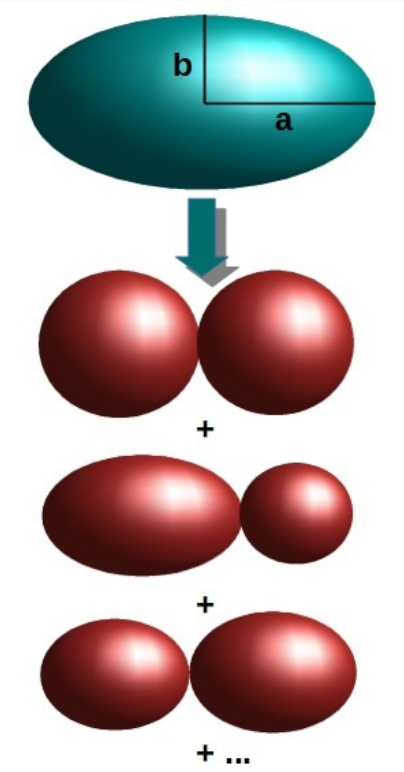

$Q_2 \sim Q_2^{ellips} \pm 10\%$

- **Probability of each DNS**

$$P_0(n) \sim \rho(n, E^* = U_{comp} - U_{DNS})$$

- **Quadrupole moment of DNS**

$$Q_2(n) = 2\frac{A_1 A_2}{A} R^2 + Q_2(A_1, \beta_1) + Q_2(A_2, \beta_2)$$

Various calculations show that nucleus can be presented as a DNS around $Q_2^{ellips} \sim 3 : 1$.

S. Cwiok, W. Nazarewicz et al., PLB, **322**, 304 (1994).
T. M. Shneidman et al., NPA, **671**, 119 (2000).
A. V. Afanasjev et al., Phys. Scr. **93**, 034002 (2018).

Fission observable distributions: A, Z, TKE

The distribution of primary fission fragments:

$$P_f(n[Z_1, A_1, \beta_1, Z_2, A_2, \beta_2])$$

The mass $Y(A)$ and charge $Y(Z)$ distributions:

$$Y(A) = \sum_{n_j} P_f(n_j) \left[\delta_{A_1,A} + \delta_{A_2,A}\right]$$

$$Y(Z) = \sum_{n_j} P_f(n_j) \left[\delta_{Z_1,Z} + \delta_{Z_2,Z}\right]$$

TKE of primary fission fragments is defined as the interaction energy at the top of the barrier $R = R_b$:

$$TKE_n = V_C(n[Z_{1,2}, A_{1,2}, \beta_{1,2}, R_b]) + V_N(n[Z_{1,2}, A_{1,2}, \beta_{1,2}, R_b])$$

Then the TKE distribution: is calculated by summing over the probabilities $P_f(n)$ corresponding to the states with TKE within a given interval 2Δ:

$$Y(TKE) = \sum_j P_f(n_j)\Theta(|TKE_{n_j} - TKE| \leqslant \Delta)$$

Neutron multiplicity

After decay of DNS, fragments shrinks to their ground state releasing its deformation energy:

$$E_i^{def}(n) = \left[U_i^{LD}(Z_i, A_i, \beta_i) + E_i^{sh}(Z_i, A_i, \beta_i)\right] - \left[U_i^{LD}(Z_i, A_i, \beta_i^{gs}) + E_i^{sh}(Z_i, A_i, \beta_i^{gs})\right]$$

Excitation energies of fragments at scission:

$$\left(\frac{1}{\rho_1(\varepsilon)}\frac{d\rho_1(\varepsilon)}{d\varepsilon}\right)\Bigg|_{\varepsilon=E_1^*} = \left(\frac{1}{\rho_2(\varepsilon)}\frac{d\rho_2(\varepsilon)}{d\varepsilon}\right)\Bigg|_{\varepsilon=E_2^*} = T^{-1}.$$

Neutron multiplicity:

$$Y(\nu) = \sum_j \left[\sum_{x=1}^{\nu} F_1(x, E_1^{def}(n_j) + E_1^*(n_j)) F_2(\nu - x, E_2^{def}(n_j) + E_2^*(n_j))\right] P_f(n_j).$$

$F_{1,2}(x, E_{1,2})$ – probabilities to emit exactly x neutrons obtained using Monte-Carlo simulation. AR et al., PLB 844 (2023) 138099.

Neutron multiplicities of $Z \sim 100$ nuclei

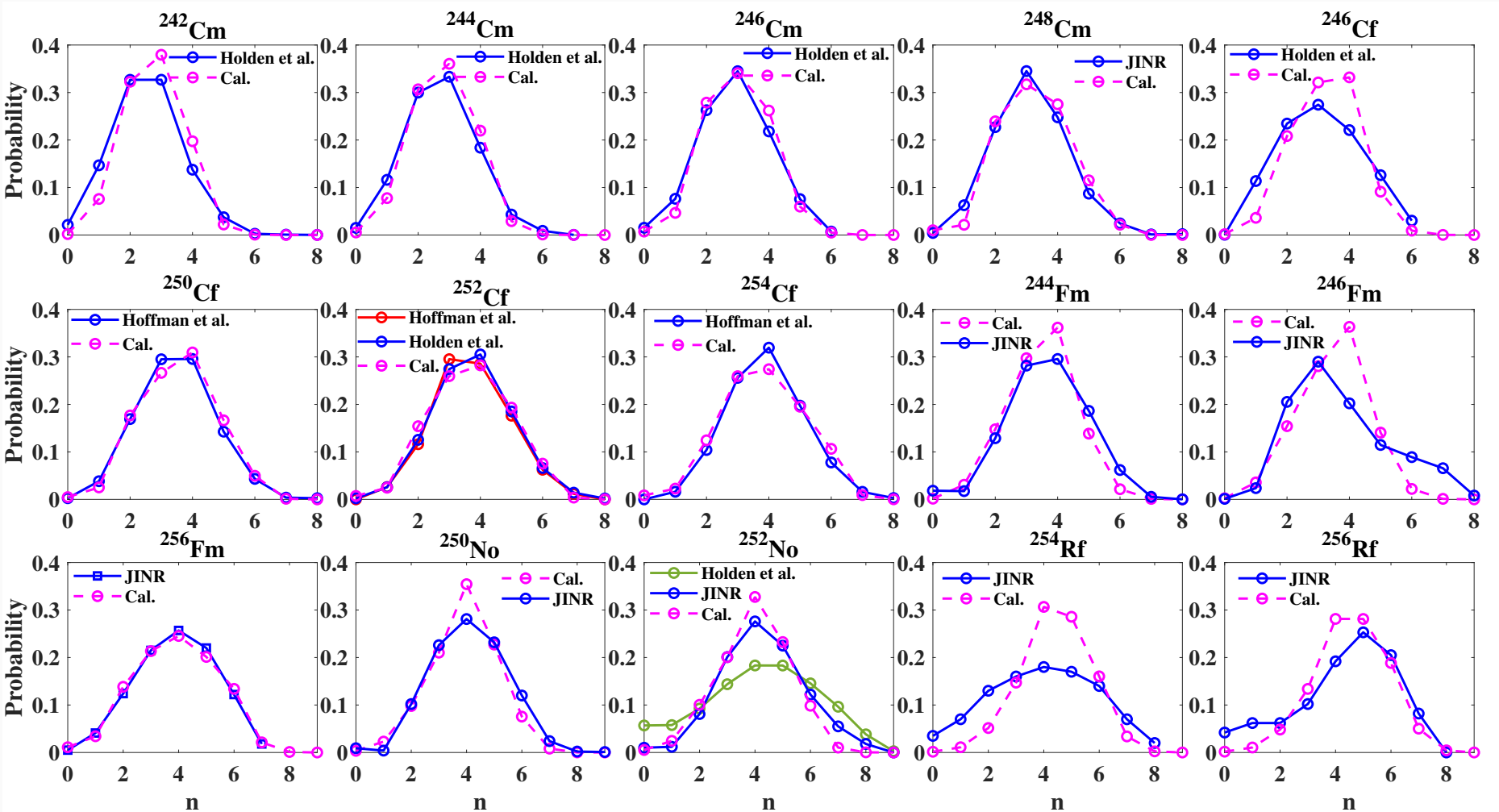

$\lambda^{(A)} = 1.7; \lambda^{(\beta)} = 1.2; Q_{init} \sim 3.2 : 1$

Evolution of DNS distribution (sample: ^{256}Rf)

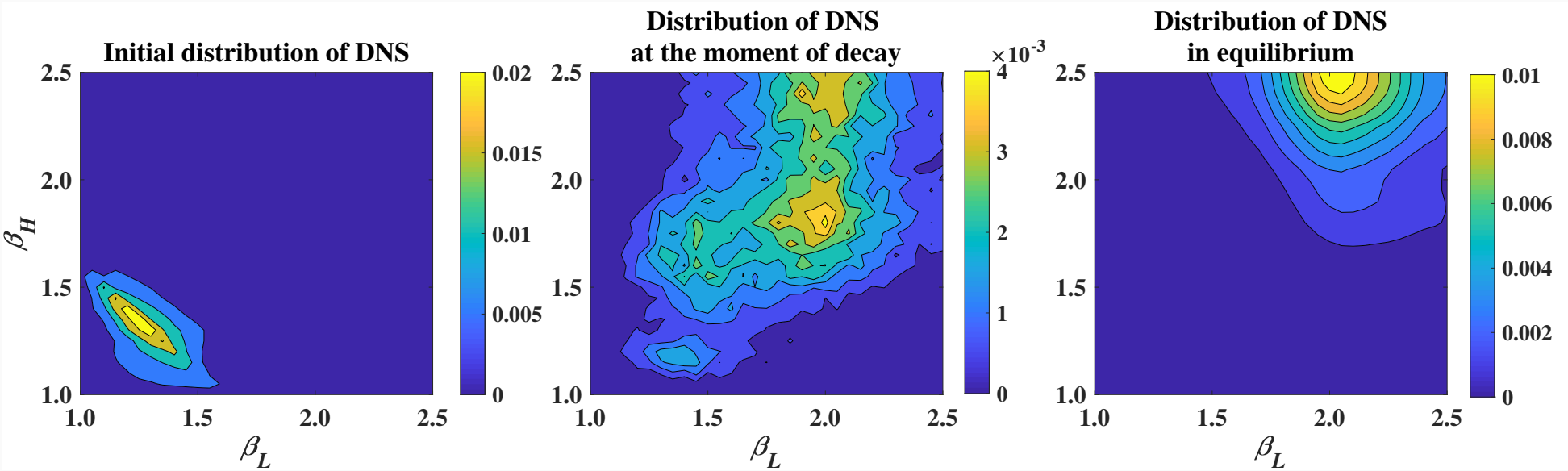

- Distribution of DNS at the moment of decay shows two wide maxima, one of which coincides with the maximum of the equilibrium distribution.
- Maximum corresponding to the compact shapes is mainly responsible for the emission of small number of neutrons.

Neutron multiplicity distributions in SF of even $^{244-260}$Fm isotopes

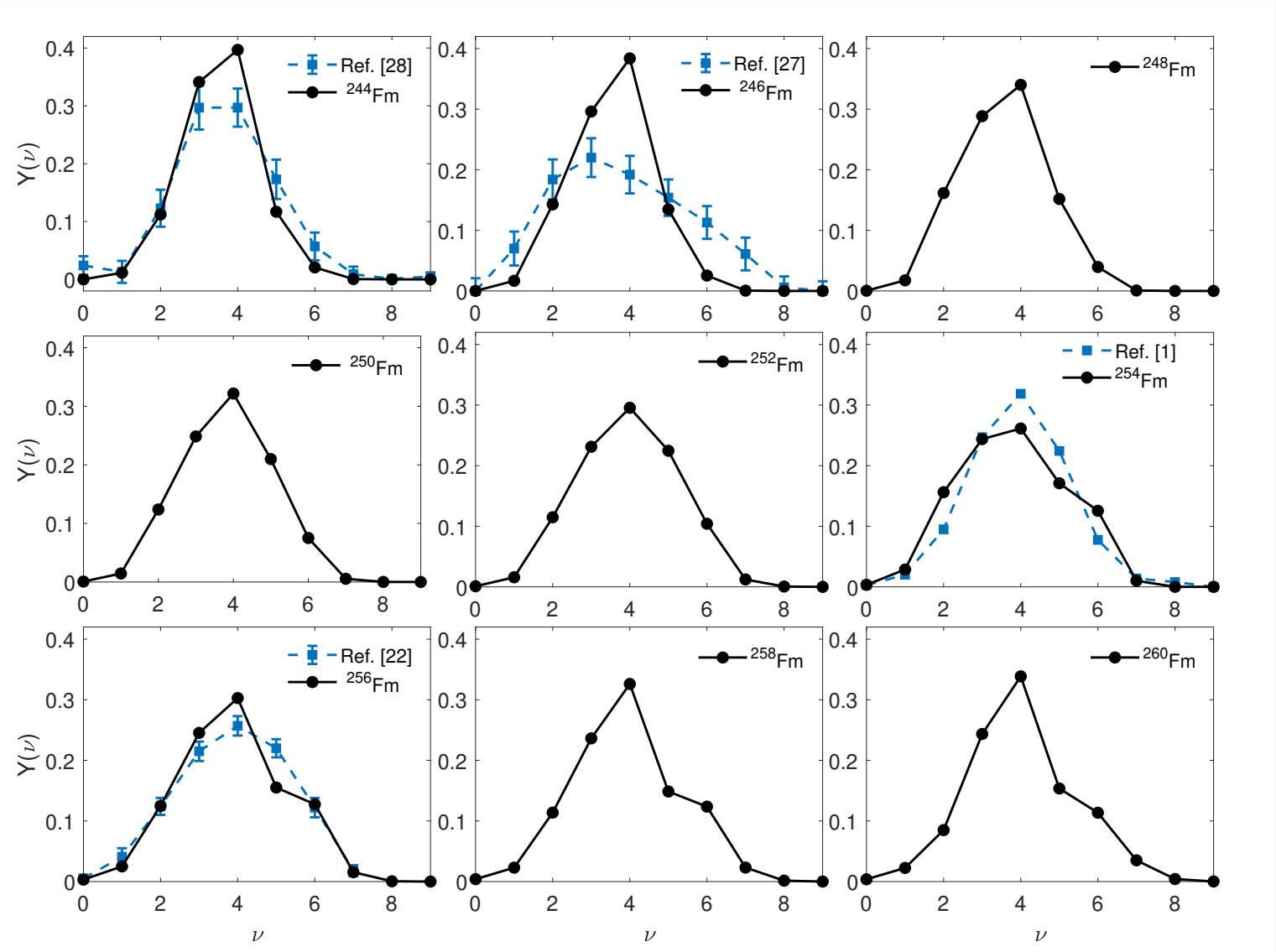

Mass distribution in SF of even $^{244-260}$Fm isotopes

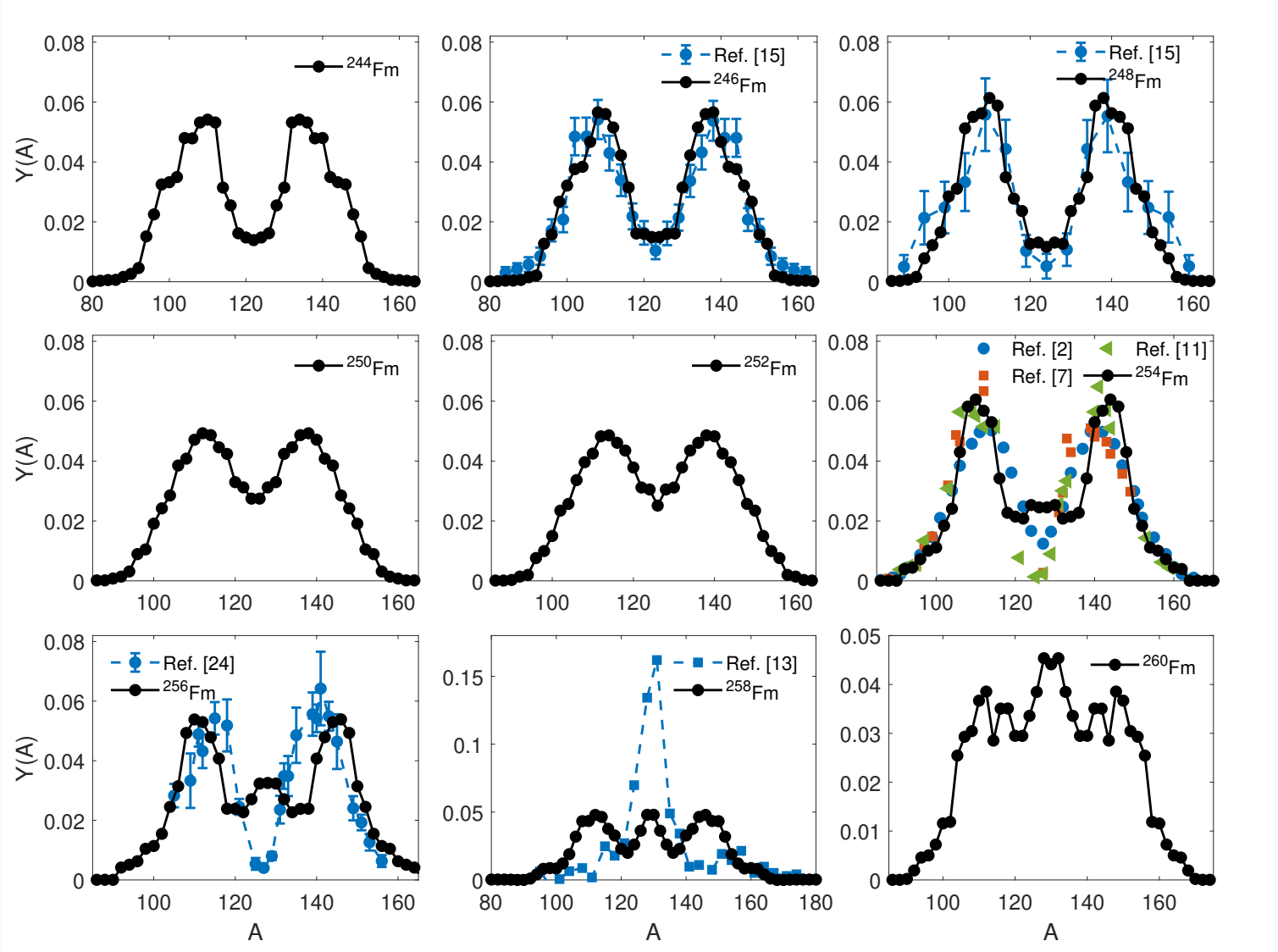

A. Rahmatinejad et al., IJMPE 33 (2024) 2441018.

Mass/Charge distribution in ^{258}Fm

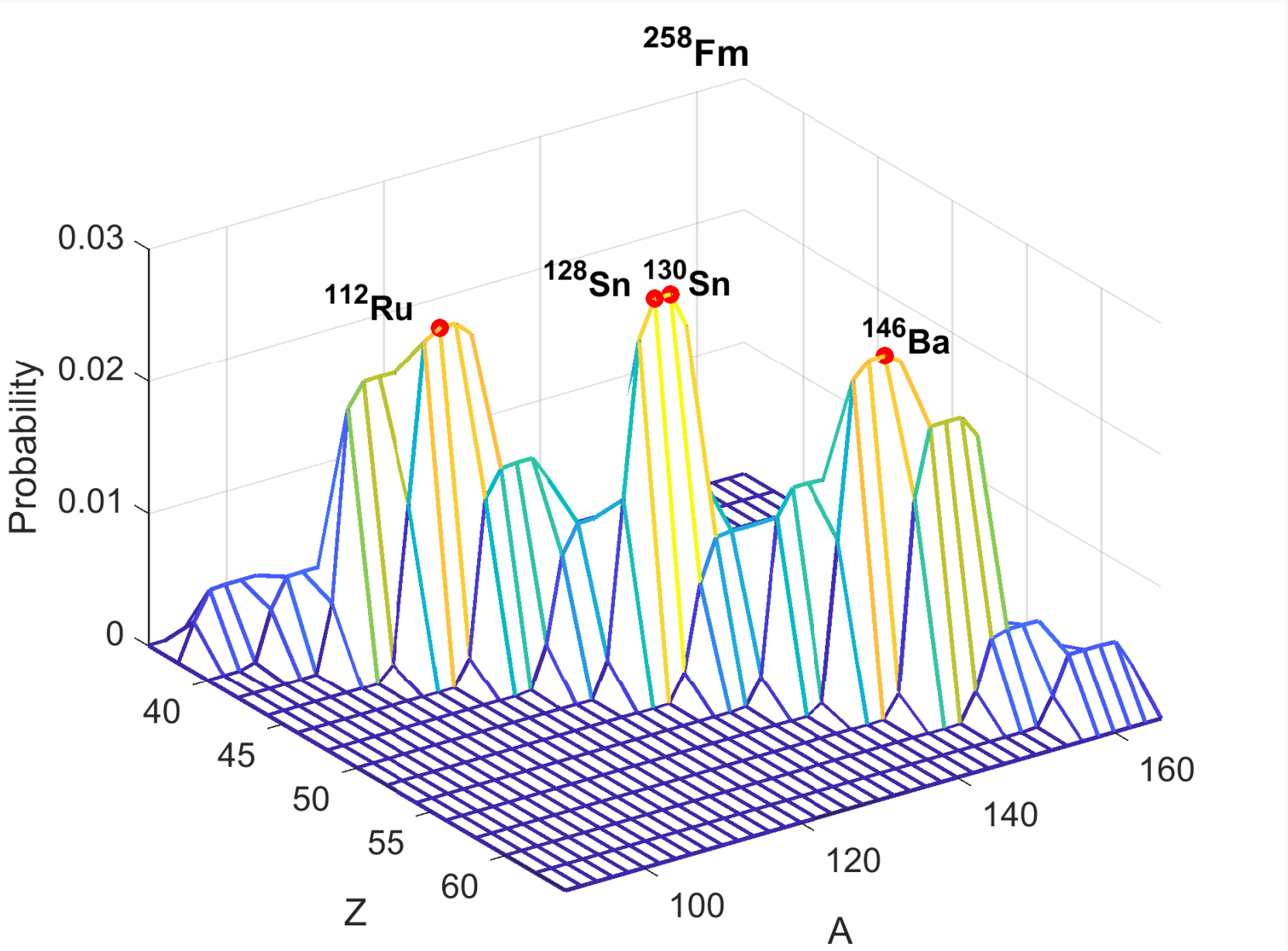

Scission configurations in SF of ^{258}Fm

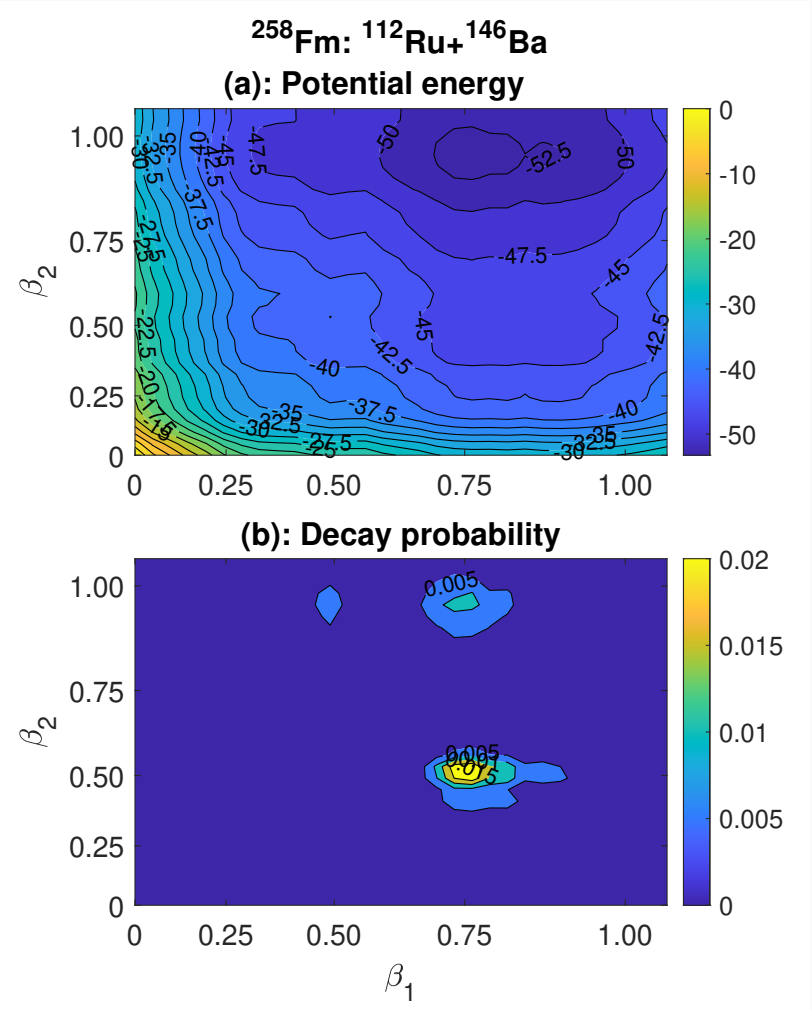

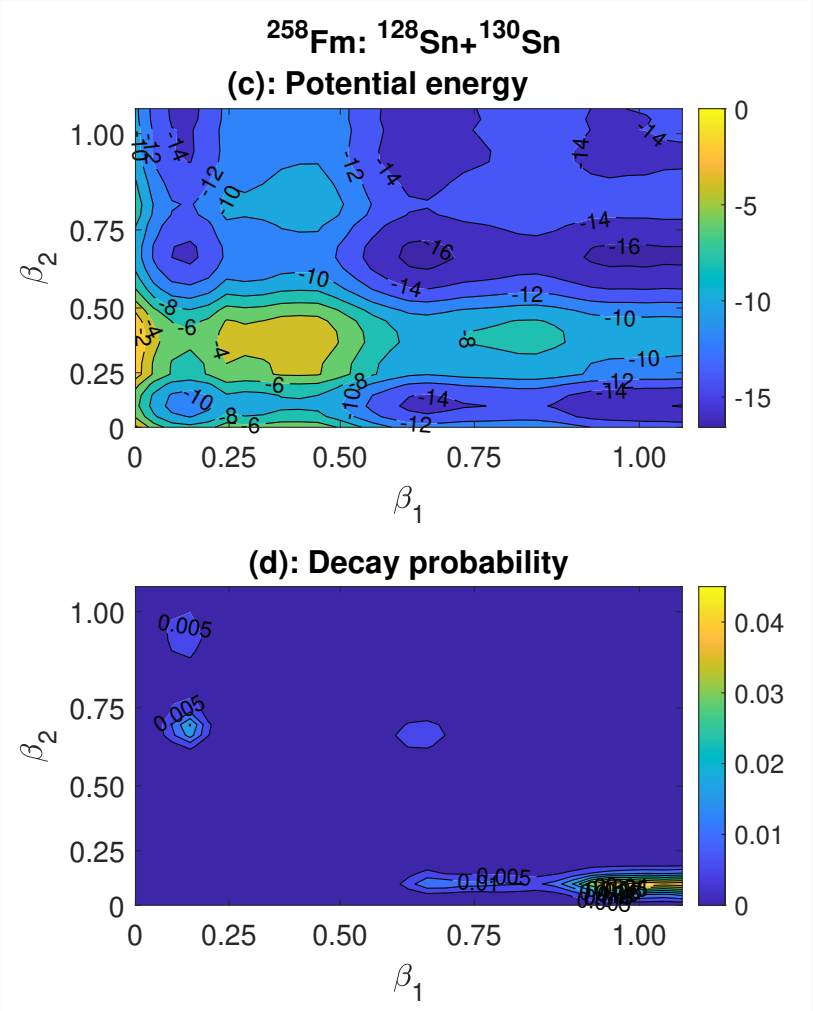

Half-lives of Fermium isotopes

Isotope	β_2 of SP	Fission barrier height (MeV)	Exp. SF half-lives
^{244}Fm	0.44	6.07	3.2165 ms
^{246}Fm	0.44	6.61	22.6471 s
^{248}Fm	0.44	6.89	9.5833 h
^{250}Fm	0.45	6.99	301.9292 day
^{252}Fm	0.45	6.98	126.0166 year
^{254}Fm	0.45	6.21	228.0417 day
^{256}Fm	0.45	5.40	2.8491 h
^{258}Fm	0.41	4.82	370 μs
^{260}Fm	0.57	4.55	-
^{262}Fm	0.57	4.74	-

Fission barriers: P. Jachimowicz, et al., ADNDT **138**, 101393, (2021).

Half lives: www.nndc.bnl.gov/ensdf.

Super-short fission mode: M. Albertsson, et al., PRC **104**, 064616 (2021).

Compact SF of ^{258}Fm

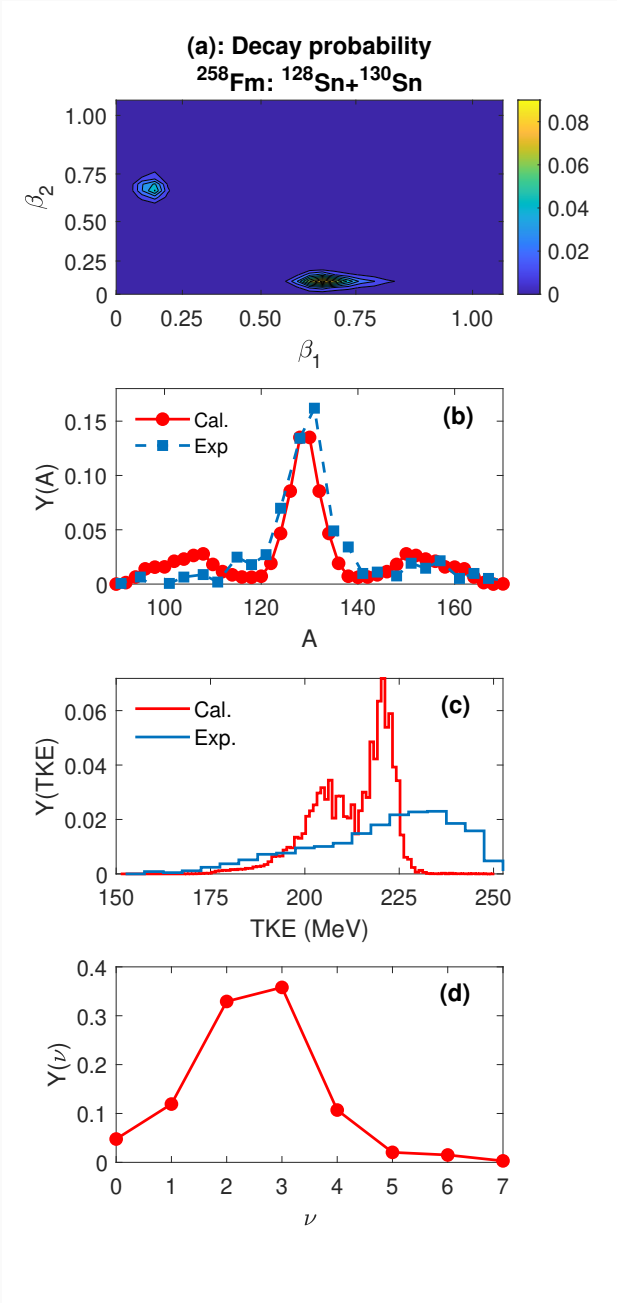

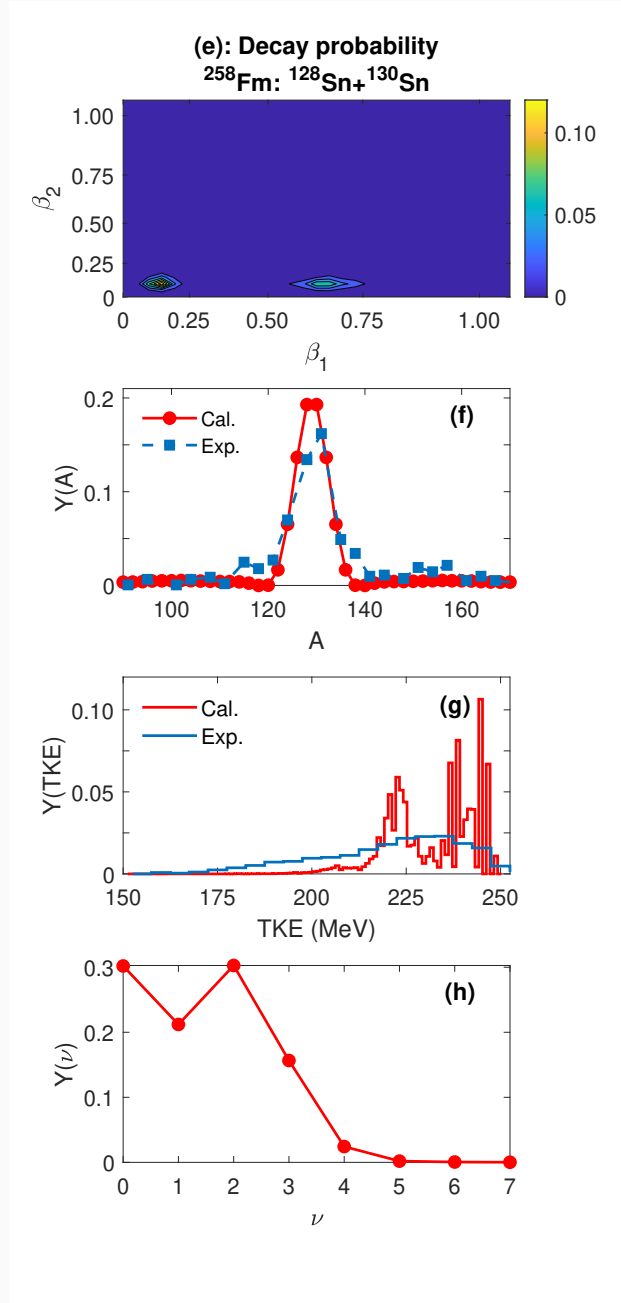

Exp. data:
D. C. Hoffman et. al, PRC, **21**, 972 (1980).
E. K. Hulet et. al, PRC **40**, 770 (1989).

Spontaneous fission of ^{258,260}Sg and ^{260}Rf

Recently, experimental study of neutron multiplicities of ^{258,260}Sg and ^{260}Rf nuclei has been carried out using the SHELLS velocity filter.

- ^{258}**Sg** was produced in: ^{207}Pb+^{52}Cr

$$\bar{\nu} = 4.9 \pm 0.4, T_{1/2} = 2.2^{+2.4}_{-1.0}\ \mathrm{ms}$$

- ^{260}**Sg** was produced in ^{207}Pb+^{54}Cr.

$$\bar{\nu} = 5.03 \pm 0.14, T_{1/2} = 7.0^{+2.6}_{-1.7}\ \mathrm{ms}$$

JINR preprint: E7-2026-3

\https://www.researchgate.net/publication/401424789_Prompt_neutron_emission_in_the_spontaneous_fission_of_258260Sg

- ^{260}**Rf** was produced in complete fusion reaction ^{238}U+^{26}Mg.

$$\bar{\nu} = 4.88 \pm 0.24, T_{1/2} = 16.8^{+5.5}_{-3.8}\ \mathrm{ms}$$

JINR preprint: E7-2026-18

https://www.researchgate.net/publication/404345430_Average_number_of_prompt_neutrons_in_the_spontaneous_fission_of_260Rf

Neutron multiplicity distributions in SF of ^{260}Sg and ^{260}Rf

^{260}Sg

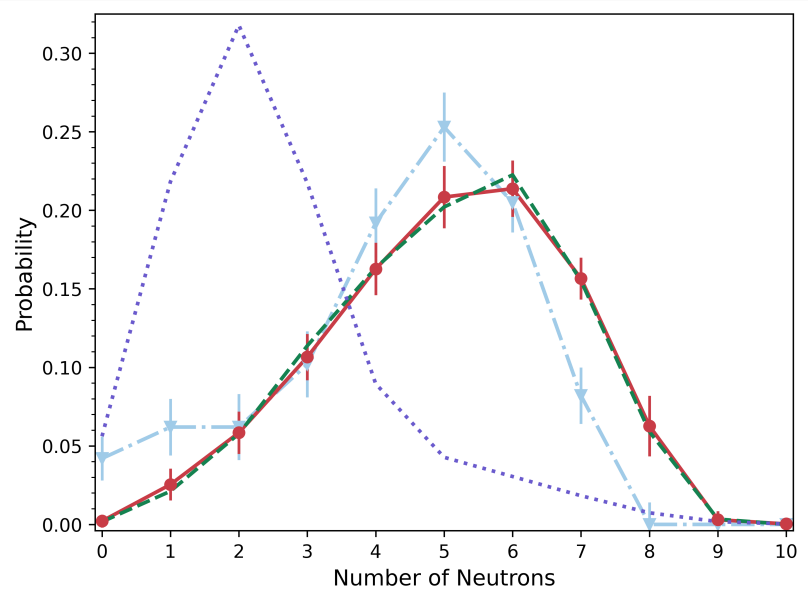

^{260}Rf

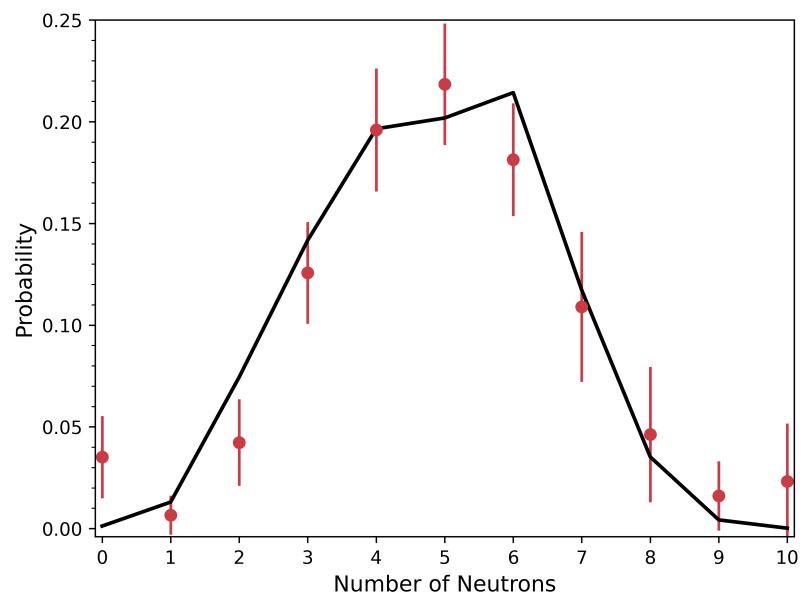

Charge/Mass distributions in SF of ^{260}Sg

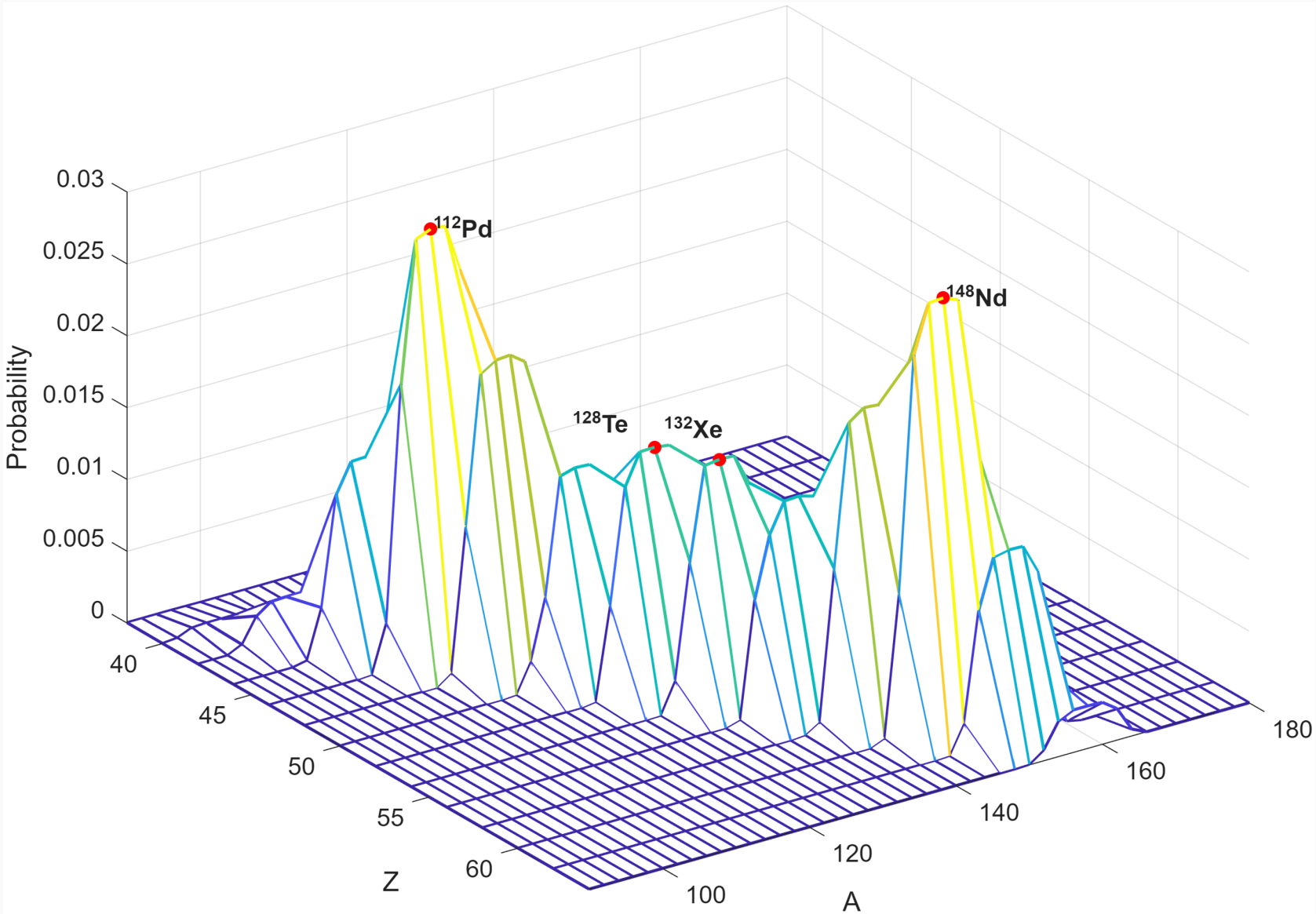

Mass and TKE distributions in SF of ^{260}Sg

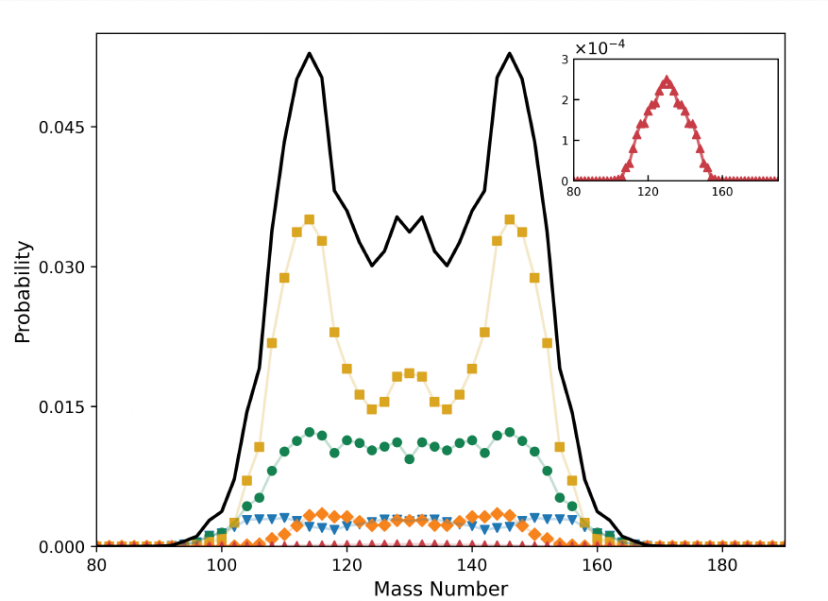

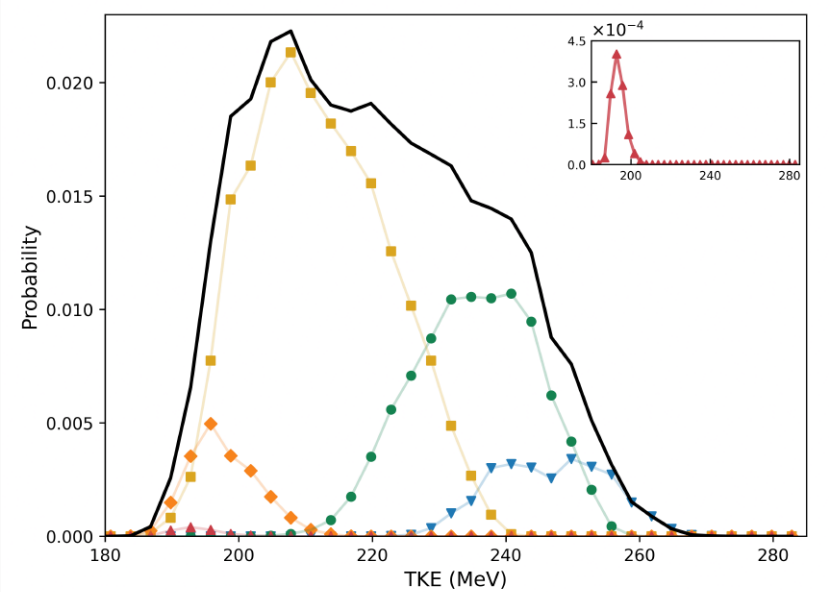

blue triangles: $\nu \leq 2$

green circles: $3 < \nu \leq 4$

yellow squares: $5 < \nu \leq 7$

orange diamonds: $\nu = 8$

red triangles: $9 < \nu \leq 10$

Decay distribution for symmetric/asymmetric mass split for SF of ^{260}Sg

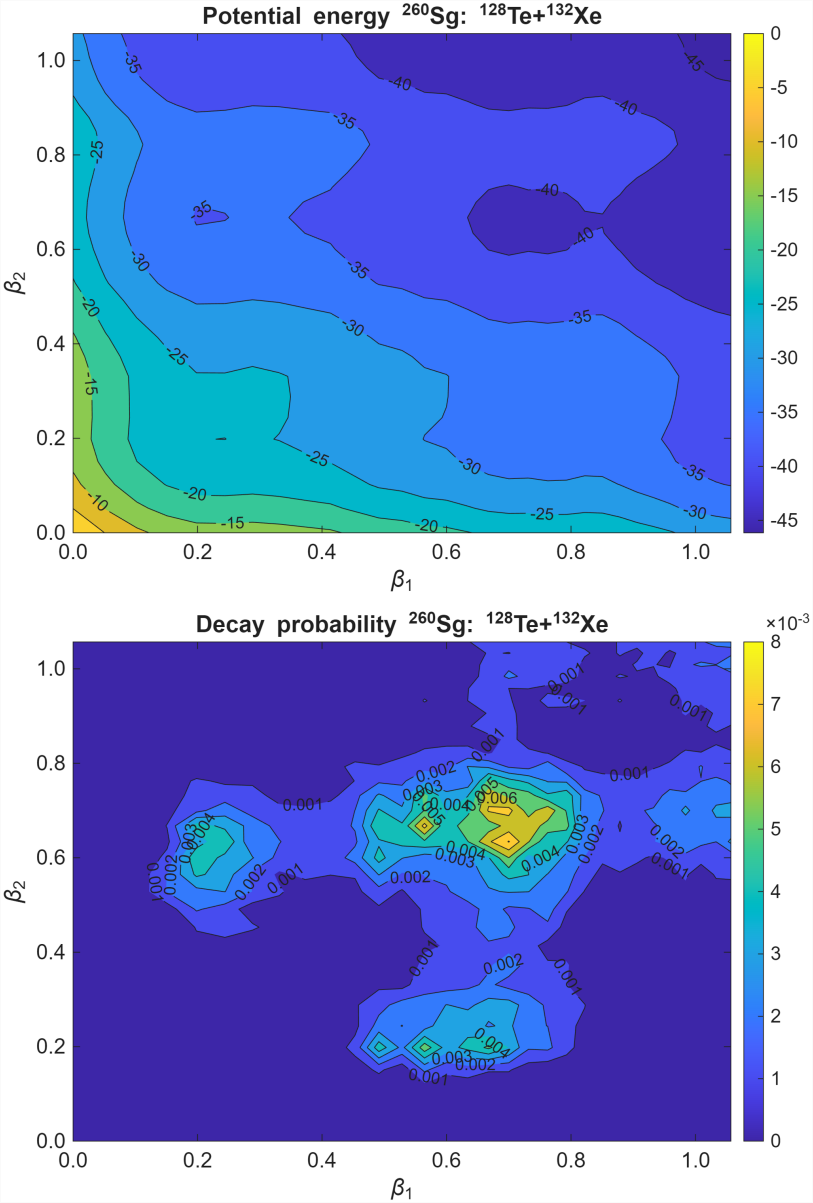

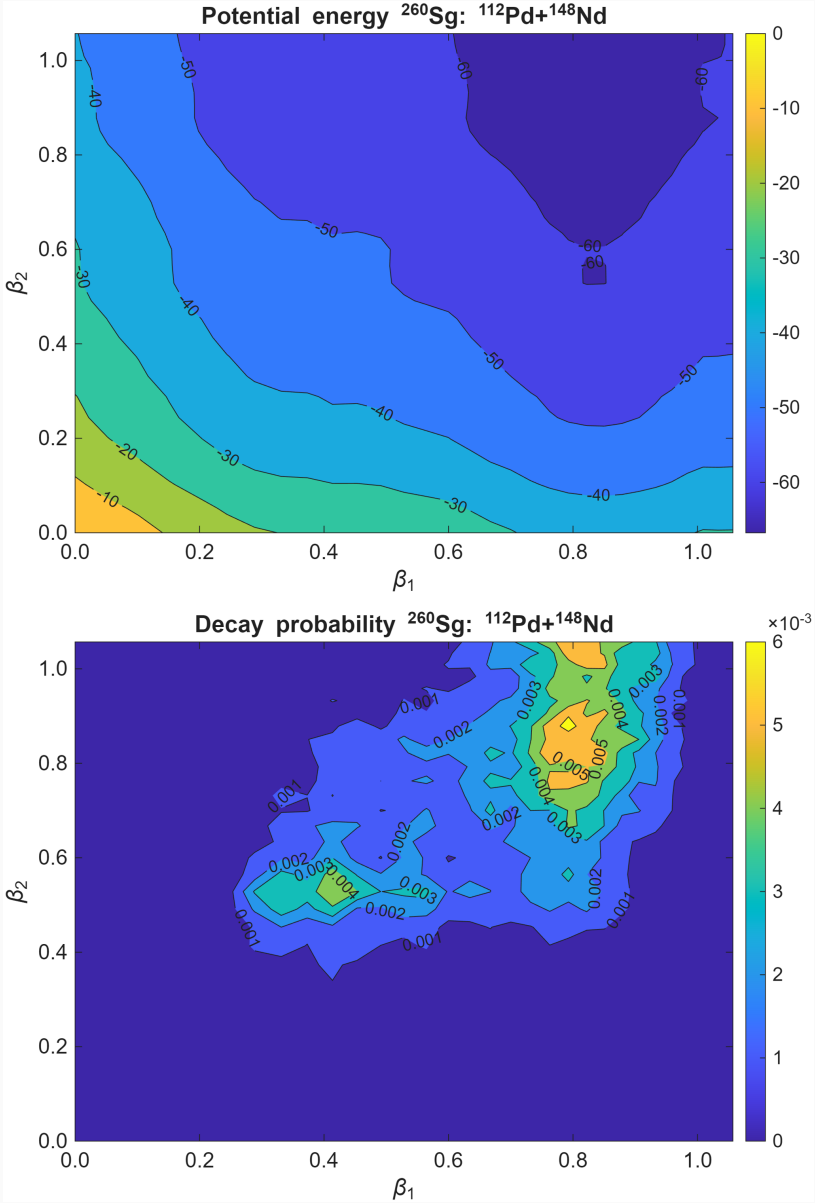

Mass distributions in SF of ^{260}Rf

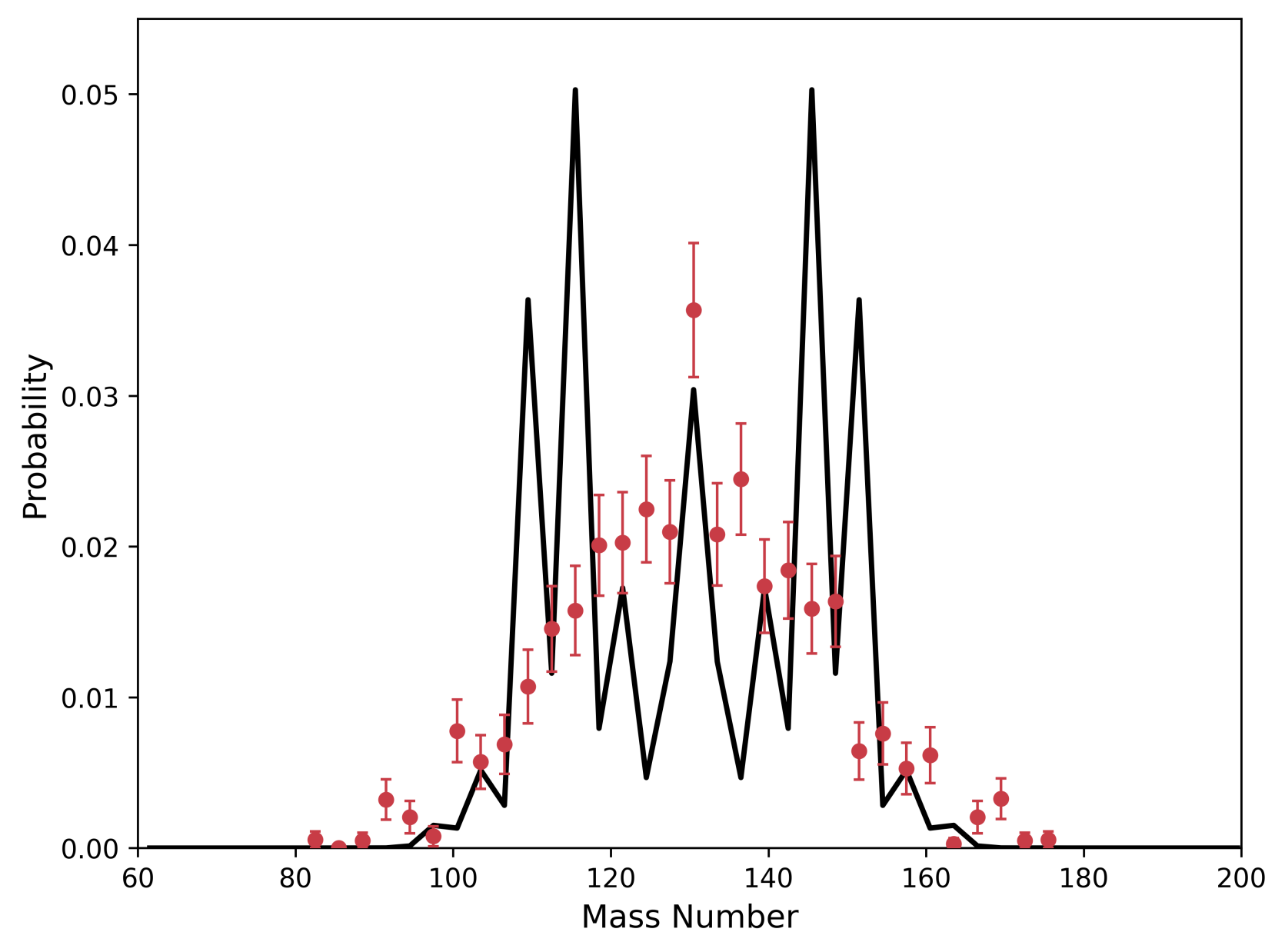

TKE in SF of ^{260}Rf

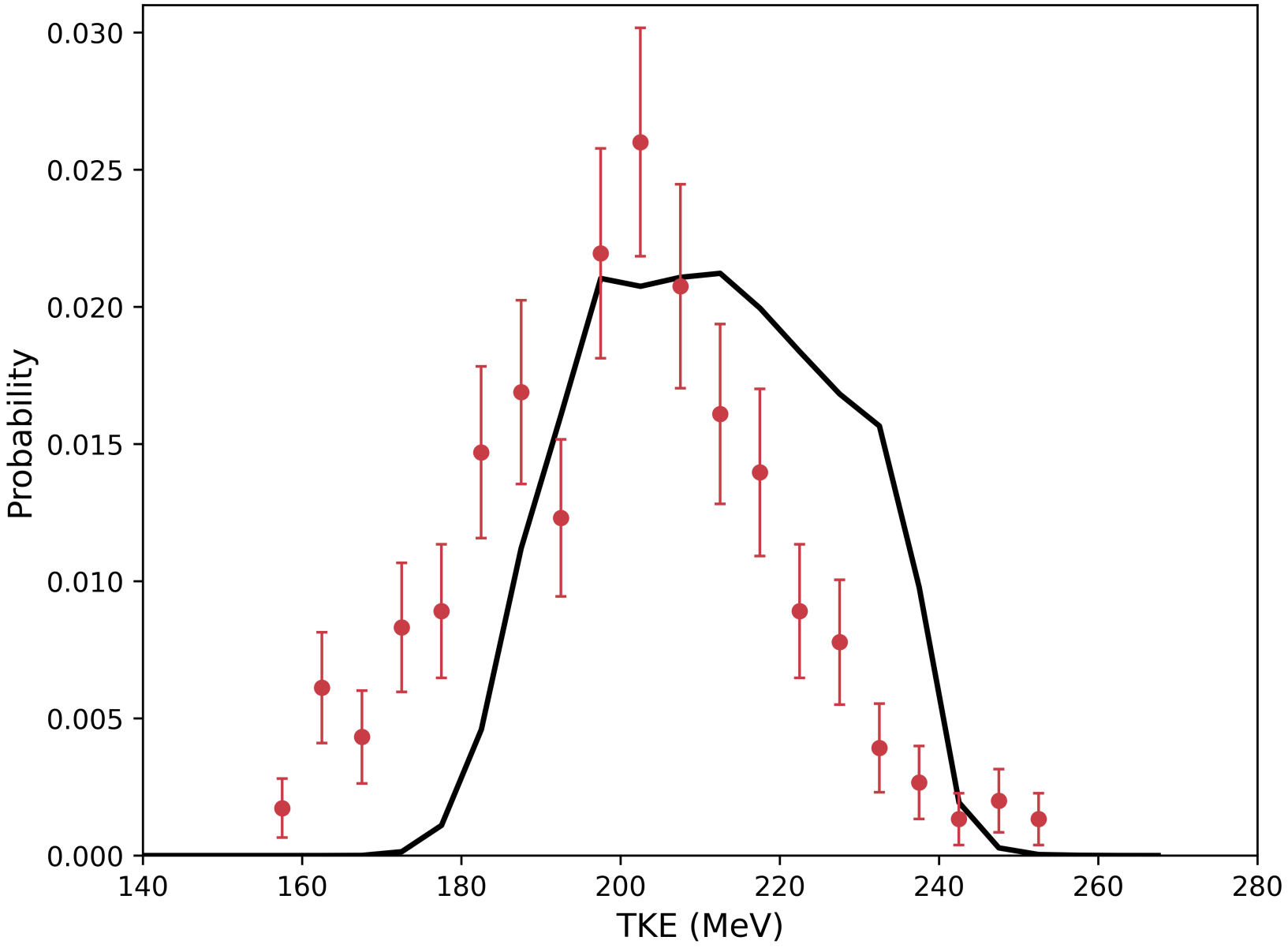

Decay distribution for symmetric mass split for SF of ^{260}Rf

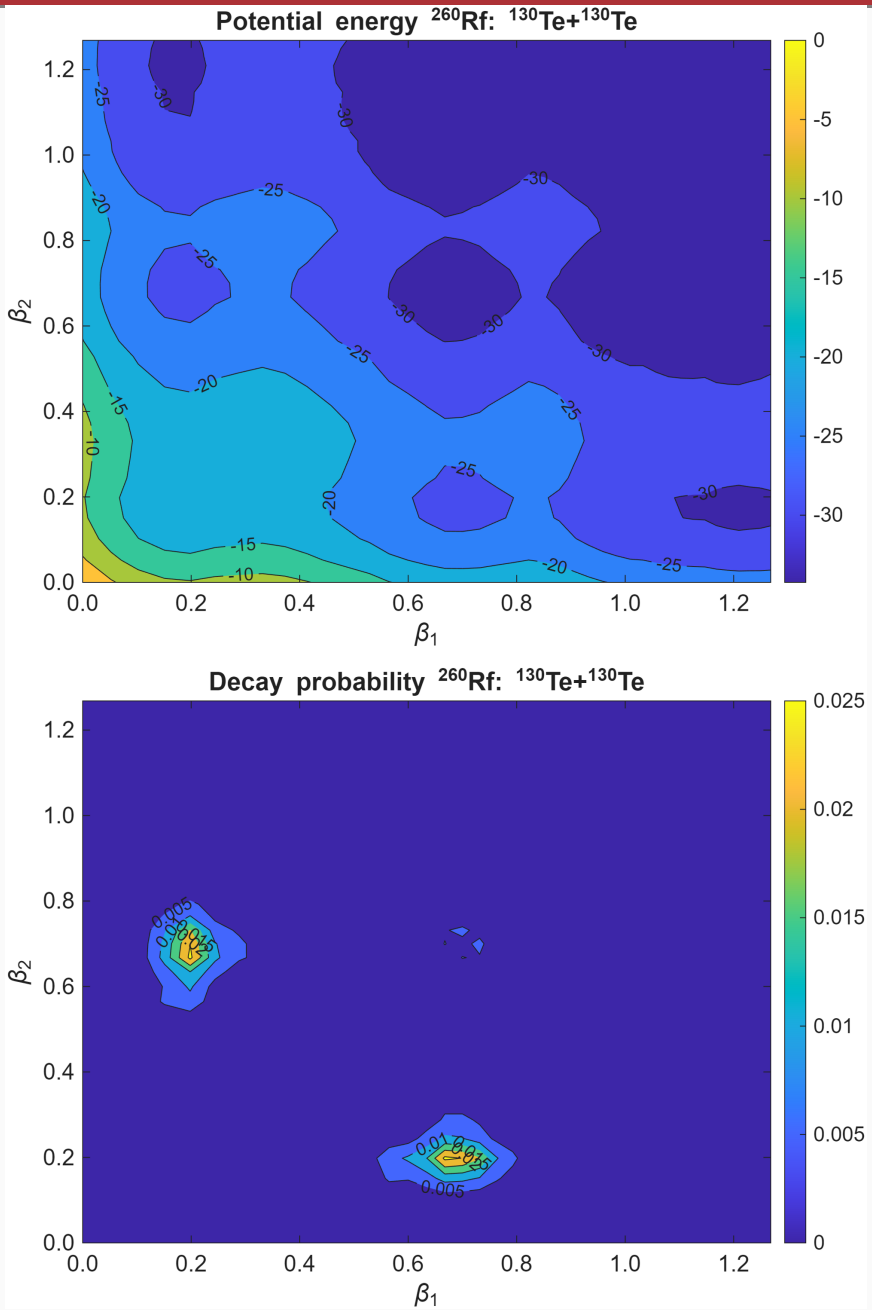

Compact symmetric fission mode:
Importance of reflection asymmetric deformation of fragments (octuple or formation of $\alpha-$cluster in the neck regions)

Conclusion

- The model to describe the evolution of a fissioning nucleus after tunneling through the fission barrier as a random walk among various dinuclear configurations is proposed.
- The prompt neutrons yield data from spontaneous fission of Z = 100–106 is described.
- Calculations of fission observables for ^{258}Fm nuclei indicate presence of bimodality due to competition between spherical (compact) and deformed mass symmetric fission modes.
- Octupole deformation of fragments is important for the description of the compact symmetric fission mode in SF of $102 \leqslant Z \leqslant 108$ nuclei.